GSI

GSI-Preprint-96-37
August 1996

DIPHOTON RATES FROM THERMALIZED MATTER RESULTING IN ULTRA-RELATIVISTIC HEAVY-ION COLLISIONS

M. HENTSCHEL, B. KÄMPFER, O. P. PAVLENKO, K. REDLICH, G. SOFF

Gesellschaft für Schwerionenforschung mbH
Planckstraße1 • D-64291 Darmstadt • Germany
Postfach 110552 • D-64220 Darmstadt • Germany

Diphoton rates from thermalized matter resulting in ultra-relativistic heavy-ion collisions

M. HENTSCHEL[1], B. KÄMPFER[1,2], O.P. PAVLENKO[2,3],
K. REDLICH[4,5], G. SOFF[1]

[1]Institut für Theoretische Physik, TU Dresden,
01062 Dresden, Germany

[2]Forschungszentrum Rossendorf, Institut für Kern- und Hadronenphysik,
PF 510119, 01314 Dresden, Germany

[3]Institute for Theoretical Physics, 252143 Kiev - 143, Ukraine

[4]Institute for Theoretical Physics, University Wrocław, 50204 Wrocław, Poland

[5]GSI, PF 110552, 64220 Darmstadt, Germany

Abstract

Diphoton radiation off strongly interacting matter resulting from ultrarelativistic heavy-ion collisions is estimated for SPS and RHIC conditions. At SPS energies the thermal diphoton signal competes strongly with the Drell - Yan like background. For given charged-particle rapidity density a scenario with deconfinement transition predicts a larger diphoton yield than a scenario without phase transition. For RHIC energies we find that radiation from initially undersaturated (but gluon-rich) deconfined matter overwhelms the hadron gas and the Drell - Yan like diphotons in the invariant mass window $1 < M < 2.5$ GeV. Due to this the so-called $M_\perp$ scaling is approximately obtained and can serve as additional tool for discriminating radiation from quark-gluon matter.

PACS: 25.75.+r; 12.38.Mh; 24.85.+p

1 Introduction

Electromagnetic signals (leptons and photons) can leave nearly undisturbed a finite system of strongly interacting matter. Therefore, despite of the low production cross sections, the dileptons and photons are considered as useful probes of the dynamics of heavy-ion collisions. It is expected that the electromagnetic radiation of highly excited matter, produced in high-energy nuclear collisions, can be sensitive to the deconfinement or chiral symmetry restoration phase transition. The recent dilepton and photon experiments at CERN-SPS [1, 2, 3] have triggered an avalanche of interpretations [4, 5, 6, 7, 8]. It is conceivable that the soft dilepton enhancement measured recently by the CERES collaboration [1, 2] could already signal the remnant of chiral symmetry restoration [5, 6]. It is, however, not excluded that other more conventional mechanisms could also be important here [8].

In the present work we would like to put particular attention for another electromagnetic probe of strongly interacting matter, namely diphotons. Such photon pairs are in many respects similar to dileptons. As it has been emphasized in ref. [9], the diphotons exhibit the appealing feature that, at given temperature, their emission rate in the deconfined phase is stronger than the rate in a hadron gas. However, in the simplified Bjorken scenario this advantage does not become operative due to the very long life time of the hadron stage after hadronization of initially deconfined thermalized matter [10]. In the mean time the importance of the transverse expansion, which shortens the life time of the hadron stage, has been recognized [11, 12, 13]. In this line, refs. [14, 15] advocate diphotons still as useful as dileptons. In addition, for very high beam energies, envisaged at RHIC and LHC, the various transport codes predict rather fast thermalization of parton matter, however, this parton matter is likely to be far from chemical equilibrium and undersaturated [16, 17]. Particle production processes via inelastic reactions also shorten the total life time of the thermalized matter. As new aspect one has further to recall that recent QCD lattice results [18] show an equation of state with much less latent heat at deconfinement than estimated within the bag model.

It seems therefore worthwhile to reconsider the diphoton rates within a hydrodynamical evolution scenario for thermalized matter which includes chemical equilibration processes on the parton level and transverse expansion, and which is capable to handle also an equation of state with reduced latent heat and a realistic description of the hadronic matter.

In this respect we also remember that the CERES and WA80/93/98 collaborations at CERN measure with detector systems which can provide us interesting diphoton data. The discrimination of background from π^0 and η^0 and other hadronic decays could proceed by the well-probed strategy as utilized in searches for direct diphotons in hadronic reactions [19].

Here we focus on the invariant mass spectra above 1 GeV (thus excluding light particle decay contributions) and analyze both the invariant mass and the transverse momentum spectra of photon pairs. It should be stressed that the elementary cross sections which we employ allow also for the calculation of relative momentum spectra. Such spectra include the proper symmetrization of the 2-photon wave function and might be considered as useful examples for intensity interferometry [20]. We plan to address the capability of this approach to the Hanbury-Brown - Twiss effect in a separate work.

Our paper is organized as follows. In section 2 we discuss the diphoton cross sections. The space time evolution of thermalized matter and the corresponding diphoton rates are presented in section 3. The spectra are displayed in section 4 for SPS and RHIC energies. The discussion and the summary can be found in section 5.

2 Diphoton cross sections

Earlier estimates of diphoton emission from equilibrium quark-gluon plasma [9, 10, 14, 15, 21] have considered only the lowest-order electromagnetic fusion process $q\bar{q} \to \gamma\gamma$. In a chemical off-equilibrium (i.e., gluon-enriched and quark - anti-quark undersaturated) plasma the process $gg \to \gamma\gamma$ can become as well important, thus it will be included in our consideration. The rate of diphoton production per space-time volume and four-momentum of the pair can be obtained within kinetic theory as

$$\frac{dN_{\gamma\gamma}^{(i)}}{d^4x\, d^4Q} = \int \frac{d^3p_1}{(2\pi)^3}\frac{d^3p_2}{(2\pi)^3} f_1(p_1,x)\, f_2(p_2,x)\, v\, \sigma^{(i)}(M^2)\, \delta^{(4)}(p_1+p_2-Q). \qquad (1)$$

where the four-momentum is $Q^\mu = (M_\perp \mathrm{ch}Y, M_\perp \mathrm{sh}Y, \vec{q}_\perp)$ with $M_\perp = \sqrt{M^2+q_\perp^2}$ as transverse mass and M as invariant mass of the $\gamma\gamma$ pair. The quantities $f_a(p_a,x)$ denote the parton (quark, anti-quark, gluon) distribution functions of species a with four-momentum $p_a^\mu = (E_a, \vec{p}_a)$. The relative velocity of the incoming partons reads $v = M/\sqrt{2E_1E_2}$. The index i specifies the $\gamma\gamma$ production process with corresponding cross section $\sigma^{(i)}$.

For massless partons the cross sections $\sigma^{(i)}$ in eq. (1) are infrared divergent. For an equilibrium quark-gluon plasma the resumation technique of Braaten and Pisarski can

be applied to regularize the rate (1), as done, e.g., in refs. [22, 23] for the single photon rate and in ref. [21] for the diphoton rate. For a chemical off-equilibrium plasma and for arbitrary invariant masses this problem requires further separate investigations since the Braaten - Pisarski technique can not be applied directly for the chemical non-equilibrium momentum distribution [24]. Otherwise, many-body effects in the QCD plasma certainly give rise to the appearance of a finite effective thermal parton mass which can account also for non-perturbative effects [25]. Such an effective mass can play a rôle of a cut-off parameter k_c which acts as regulator of the cross sections $\sigma^{(i)}$. We employ for our purposes a suggestion of refs. [23, 24] and take $k_c^2 = 2m_{th}^2(T)$ with $m_{th}^2(T) = \frac{4}{9}(\lambda_g + \frac{1}{2}\lambda_q)\pi\alpha_s T^2$ [17] being the thermal quark mass. The parton fugacities $\lambda_a = \lambda_{q,\bar{q},g}$ measure the degree of phase space saturation. Here, charge symmetry is explicitly assumed, i.e., $\lambda_q = \lambda_{\bar{q}}$. In chemical equilibrium the fugacities become $\lambda_a = 1$ and the phase space is fully saturated. Inserting this cut-off parameter k_c^2 in the t channel scattering diagrams one yields for $k_c^2 \ll M^2$

$$\begin{aligned} \sigma^{q\bar{q}\to\gamma\gamma}(M^2) &= 4N_c^2\frac{1}{2}\left(\sum_q e_q^4\right)\int_{-s+k_c^2}^{-k_c^2} dt\left(\frac{d\sigma}{dt}\right)^{q\bar{q}\to\gamma\gamma} \qquad (2)\\ &\approx 4N_c\left(\sum_q e_q^4\right)\frac{2\pi\alpha^2}{M^2}\ln\frac{M^2-k_c^2}{e\,k_c^2}, \end{aligned}$$

$$\sigma^{gg\to\gamma\gamma}(M^2) = 4(N_c^2-1)^2\frac{1}{2}\int_{-s+k_c^2}^{-k_c^2} dt\left(\frac{d\sigma}{dt}\right)^{gg\to\gamma\gamma}, \qquad (3)$$

where $s = M^2$, $\alpha = 1/137$, $N_c = 3$ is the numbers of colors, $\sum_q e_q^4 = \frac{17}{81}$ for u,d quarks, and the strong coupling constant $\alpha_s = 0.3$ is employed in our calculations. The differential cross section $(d\sigma/dt)^{gg\to\gamma\gamma}$ in the order $\alpha^2\alpha_s^2$ is taken from ref. [26][1], with the corresponding additional factors related to the summation over initial color and spin states and $\frac{1}{2}$ to avoid a double counting in the entrance channel.

The cross section $\sigma^{q\bar{q}\to\gamma\gamma}$ differs from the vacuum cross section $\sigma_{m_q^0}^{q\bar{q}\to\gamma\gamma}$ [9, 10] and the *ad hoc* regularized one $\sigma_{m_{th}}^{q\bar{q}\to\gamma\gamma}$ [15] as well as from the properly regularized one $\sigma_T^{q\bar{q}\to\gamma\gamma}$ [21] in case of full phase space saturation. It turns out that $\sigma_{m_q^0}^{q\bar{q}\to\gamma\gamma} > \sigma_{m_{th}}^{q\bar{q}\to\gamma\gamma} > \sigma^{q\bar{q}\to\gamma\gamma} > \sigma_T^{q\bar{q}\to\gamma\gamma}$. A comparison of the cross section $\sigma^{q\bar{q}\to\gamma\gamma}$ with $\sigma_{m_q^0}^{q\bar{q}\to\gamma\gamma}$ and $\sigma_T^{q\bar{q}\to\gamma\gamma}$ is displayed in fig. 1 for various temperatures. As can be observed in fig. 1 the cross sections differ substantially at smaller invariant mass, in particular at high temperature, while for larger values of M the difference becomes moderate. Note that $\sigma^{q\bar{q}\to\gamma\gamma}$ depends also on the fugacities

[1] Eq. (7.1.53) with a correction in line 6 for a misprint to preserve the $\hat{t} \leftrightarrow \hat{u}$ symmetry.

via the cut-off parameter k_c: phase space undersaturation diminishes the screening and causes an increase relative to $\sigma_T^{q\bar{q}\to\gamma\gamma}$, i.e., at high temperatures and small values of $\lambda_{q,g}$ the suppression due to screening will not be so strong as displayed in figs. 1b and c. The cross section $\sigma^{q\bar{q}\to\gamma\gamma}$ is larger by a factor 15 - 25 than $\sigma^{gg\to\gamma\gamma}$, see fig. 1. Nevertheless, since initially $\lambda_q \approx \frac{1}{5}\lambda_g$ is predicted in many models [16, 17] for RHIC conditions, one expects that the gluon fusion process might be as important as the quark annihilation.

We restrict our discussion only to high-energy diphotons with energy $E = Q^\mu u_\mu \gg T$ and utilize the Boltzmann approximation for all partons, i.e.,

$$f_a(p_a, x) = \lambda_a(x)\, \exp\{-\frac{p_a^\mu u_\mu}{T}\}, \tag{4}$$

where u^μ represents the flow four-velocity. This implies that the partons are assumed to be in thermal but not necessarily in chemical equilibrium. Integration over the momenta of the incoming particles in eq. (1) with the momentum distribution function (4) yields then for the diphoton rate from parton matter

$$\frac{dN_{\gamma\gamma}^{qgp}}{d^4x\, d^4Q} = \frac{M^2}{2(2\pi)^5}\, \exp\{-\frac{Q^\mu u_\mu}{T}\}[\lambda_g^2 \sigma^{gg\to\gamma\gamma}(M^2) + \lambda_q^2 \sigma^{q\bar{q}\to\gamma\gamma}(M^2)]. \tag{5}$$

The emissivity of deconfined matter due to the different parton reactions can be characterized by the rate as a function of the invariant mass

$$\frac{dN_{\gamma\gamma}}{d^4x\, dM^2} = \frac{M^3 T}{2(2\pi)^4} K_1\left(\frac{M}{T}\right) \lambda^2 \sigma^{(i)}, \tag{6}$$

where $\lambda = \lambda_q$ for quark annihilation processes with $\sigma^{(i)} = \sigma^{q\bar{q}\to\gamma\gamma}$, and $\lambda = \lambda_g$ for gluon fusion with $\sigma^{(i)} = \sigma^{gg\to\gamma\gamma}$; K_1 is here the modified Bessel function. The corresponding rates are displayed in figs. 2a and b for $\lambda_q = \frac{1}{5}\lambda_g$. Indeed, the gluon fusion process is a dominating source of $\gamma\gamma$ pairs under such conditions. In particular, at small values of M the gluon process tends to compensate the reduced (by screening) quark fusion yield and brings the rates near to the naive estimates which rely on the vacuum cross section. The cross section $\sigma_T^{q\bar{q}\to\gamma\gamma}$ and the corresponding rate calculated in ref. [21] can not be extrapolated to too low invariant mass because it was obtained under the condition $M \gg T$. Otherwise, we are interested in the region just above $M = 1$ GeV which has the best chances to be experimentally accessible and because at essentially larger invariant mass the Drell - Yan like process ultimately dominates. Therefore we prefer to employ in the present work $\sigma^{q\bar{q}\to\gamma\gamma}$.

The diphoton emission rate from the hadron gas can be expressed in close analogy to eq. (5) as

$$\frac{dN_{\gamma\gamma}^{had}}{d^4x\, d^4Q} = \frac{M^2}{2(2\pi)^5}\, \exp\{-\frac{Q^\mu u_\mu}{T}\}\, \sigma^{had}(M^2) \tag{7}$$

where the hadron cross section of the reaction $\pi^+\pi^- \to \gamma\gamma$ within the approximation $M^2 \gg m_\pi^2$ reads

$$\sigma^{had}(M^2) = \frac{4\pi\alpha^2}{M^2}[1 - \frac{4m_\pi^2}{M^2}\ln\{\frac{M^2}{m_\pi^2}\}] \tag{8}$$

(and analogously for the K^+K^- annihilation channel). This cross section results in $\sigma^{had}(M^2)\,M^2 \approx 6 \cdot 10^{-4}$ at $M > 1$ GeV. Since at high enough temperature the quark fusion cross section is much larger than the pion annihilation channel, one originally expected [9] that the diphoton signal is more useful for the deconfinement diagnostic than the corresponding dilepton signal. However, as mentioned in ref. [21] this advantages is diminished due to screening. The contribution of the K^+K^- channel is found to be small [15], thus it can not change the above conclusions.

3 Space-time evolution and diphoton yields

Until now we have analyzed the $\gamma\gamma$ rate per space-time volume and invariant mass. In heavy-ion collisions, however, the thermal medium is not a static object but rather undergoes space-time evolution. Thus one still needs to integrate the rates in eqs. (1,4,5) over the history of the collision. We adopt in our considerations the hydrodynamical model for the evolution of thermalized matter as described in refs. [11, 12]. In this model the transverse expansion is superimposed on scale-invariant longitudinal expansion; the former one is dealt with our global hydrodynamics [11], where $u_\perp = ([\partial R/\partial\tau]\,R)r$ and $u_\perp = v_\perp\gamma_\perp$ hold. Since deconfined matter is predicted to be created in a chemical off-equilibrium state [16] at RHIC energies we follow the evolution of thermalized matter by means of local rate equations. We assume such a fast equilibration that at confinement temperature the chemical equilibrium is reached, and we employ the standard procedure to follow the confinement transition of hadronizing matter. It is assumed that the contributions from the hadronic decays after freeze-out can be subtracted from experimental spectra (e.g., by invariant mass cuts), so this component is not included in our model.

The flow velocity in our approach reads

$$u^\mu = \gamma_\perp(\mathrm{ch}\eta, \mathrm{sh}\eta, \vec{v}_\perp), \quad \gamma_\perp = (1 - v_\perp^2)^{-1/2}, \tag{9}$$

which gives the diphoton energy $E = Q^\mu u_\mu = M_\perp\gamma_\perp \mathrm{ch}(Y - \eta) - q_\perp\gamma_\perp v_\perp \cos\phi$, where ϕ is the angle between the diphoton momentum $\vec{q}_\perp$ and the hydrodynamical flow velocity $\vec{v}_\perp$ in the transverse direction. The space-time volume is $d^4x = \tau d\tau\, r dr\, d\phi\, d\eta$; therefore, the

space-time integrated rate can be written as

$$\frac{dN_{\gamma\gamma}}{dM_\perp^2\, dq_\perp^2\, dY} = \frac{M^2}{4(2\pi)^3}\int_{\tau_0}^{\tau_f} d\tau\,\tau\int_0^{R(\tau)} dr\, r\, K_0\left(\gamma_\perp\frac{M_\perp}{T}\right) I_0\left(\gamma_\perp\frac{v_\perp M_\perp}{T}\right)\times$$
$$\{[\lambda_g^2\sigma^{gg\to\gamma\gamma}+\lambda_q^2\sigma^{q\bar{q}\to\gamma\gamma}]x+\sigma^{had}(1-x)\}, \qquad (10)$$

where x is the actual relative weight of deconfined matter (i.e., 1 and 0 in the deconfined and confined phase, respectively, and $0 < x < 1$ in the mixed phase). K_0 and I_0 are modified Bessel functions. The numerical integration in eq. (10) is based on the hydrodynamical scheme [11, 12] discussed above. Integrating the rate (10) over $q_\perp$ we get the invariant mass spectrum

$$\frac{dN_{\gamma\gamma}}{dM^2\, dY} = \frac{M^2}{2(2\pi)^3}\int_{\tau_0}^{\tau_f} d\tau\,\tau\int_0^{R(\tau)} dr\, r\, M\, T\, K_1\left(\frac{M}{T}\right)\{\cdots\} \qquad (11)$$

with $\{\cdots\}$ as in eq. (10).

The Drell - Yan like background $\frac{dN_{\gamma\gamma}^{DY}}{dM^2\,dY}$ is estimated with Duke - Owens structure functions, set 1.1 with K factor 2, by replacing the dilepton cross sections (cf. [12, 27]) by the free diphoton cross sections [10]. The calculation of $\frac{dN_{\gamma\gamma}^{DY}}{dM^2\,dY}$ is reliable only for large enough invariant masses. We are going to extrapolate down to have an estimate of a possible background which competes with the thermal source. For a recent discussion of the Drell - Yan process we refer to [28].

4 Spectra of diphotons

We present our results for the $\gamma\gamma$ spectra assuming initial conditions for the thermalized era which are appropriate for Pb + Pb at SPS and RHIC energies. In both cases the initial transverse radius is $R_0 = 7$ fm, corresponding to mass numbers in the region at $A \approx 200$. The initial transverse velocity is $v_\perp^0 = 0$, whereas the freeze-out is assumed to happen at $T_{f.o.} = 120$ MeV. A possible baryon chemical potential is neglected. The deconfinement temperature is fixed at $T_c = 169$ MeV.

4.1 Diphoton yield for SPS energies

Here we assume the standard initial time of the thermalized era, i.e. $\tau_0 = 1$ fm/c. We are going to consider two very different scenarios of the matter evolution: one with and another without deconfinement phase transition. In the first scenario (I) we employ the

standard bag model equation of state with massless pions below T_c. The usual estimate of the initial entropy density $s_0 = \frac{3}{2}(dN_{ch}/dY)/(0.27\pi R_0^2 \tau_0)$ yields $T_0 = 191$ MeV because $s(T) = \frac{4}{3}\frac{37}{30}\pi^2 T^3$; we rely here on the CERES average $dN_{ch}/dY \approx 410$. Since the initial time is poorly constrained and might fluctuate as dN_{ch}/dY fluctuates as well we also use $T_0 = 250$ MeV for this scenario. This latter initial temperature should be considered as an (extreme) upper bound and is motivated formally to check the sensitivity of our results against variations of T_0. In all these estimates we have assumed full phase space saturation, i.e. $\lambda_{q,g} = 1$.

The other scenario (II) is based on a model equation of state for an ideal hadron gas mixture of the first 100 lightest hadrons. This results for the charged-particle rapidity density of 410 in $T_0 = 204$ MeV, which might be considered as still acceptable value for purely hadronic matter. This temperature corresponds to a particle density of 1.8 fm^{-3}. A massless pion gas would yield $T_0 = 442$ MeV, while the inclusion of massive π, ρ, ω, η gives 310 MeV [15]; such exotically superheated hadronic matter is far non-realistic. The upper limit of the initial temperature of 250 MeV in the above scenario I translates into $T_0 = 228$ MeV for scenario II.

It is worthwhile to notice that the scenario I represents an extreme possibility of modeling the deconfinement transition: It provides the maximum contribution from the hadron stage to the diphoton spectrum at $M > 1$ GeV due to the large latent heat which gives rise to a long-living mixed phase. Another model equation of state with reduced latent heat at fixed T_c would result in a smaller contribution from the hadron stage. Accordingly we do not intend to combine the bag model with the resonance gas. The scenario II is opposite to I in the sense that it does not possess a phase transition at all.

Neglecting the baryo-chemical potential is certainly some approximation for SPS energies. Nevertheless, the measured relative abundances of mesons to baryons is $\#_{mes}/\#_B \sim 5$ in the central region at SPS energies, thus the above assumption can still be suitable. Furthermore, the suppression of the diphoton production from deconfined matter due to the finite baryon charge [29, 30] is estimated to leave essentially unchanged our conclusions.

In fig. 3 we present our main results on the diphoton spectra for the two scenarios I and II described above. The slopes of the invariant mass spectra are rather similar in both cases. This reflects the approximately equal initial temperatures of the deconfined matter and the resonance gas at fixed final charged-particle multiplicity. The different yields for scenarios I and II can be traced back to the different diphoton cross sections (see figs. 1a

and b) and different life times. It turns out that the contribution from the long-living mixed phase in scenario I dominates the yield (cf. [31] for the analog effect for dileptons). For a more realistic model with reduced latent heat the life time of the mixed phase is shortened and correspondingly the yield is decreased towards the yield in our secenario II. Therefore, the increase by a factor 3 - 5 of the yield due to the deconfinement transition in scenario I, as compared to the resonance gas yield, is not so large to be considered as safe effect which might help to discriminate experimentally deconfined matter.

One can observe in fig. 3 that the down-extrapolated Drell - Yan like background dominates at $M > 1.5$ GeV. This makes the identification of a signal from thermalized matter (independent of the onset of deconfinement) difficult, at least when using only the invariant mass spectra of diphotons. Probably more delicate characteristics like angular or relative momentum correlations of photon pairs could help here.

This conclusion is not changed even if we compare the both scenarios I and II for the above mentioned higher initial temperatures, see fig. 4. The situation looks somewhat more favorable for the thermal signal, in particular when assuming deconfinement. As mentioned above, however, it seems questionable that such high-multiplicity events, which are attributable to these large values of T_0 employed in fig. 4, can be really found at SPS energies.

4.2 Diphoton yields for RHIC energies

Our set of initial conditions appropriate for RHIC energies is characterized by the time $\tau_0 = 0.32$ fm/c, temperature $T_0 = 550$ MeV, gluon fugacity $\lambda_g^0 = 0.5$, quark fugacity $\lambda_q^0 = \frac{1}{5}\lambda_g^0$, The most prominent feature here is the phase space undersaturation; its actual value, however, is not well established. Earlier predictions gave much smaller values [16, 17], while most recent HIJING-based estimates [32] point to the values of $\lambda_{q,g}^0$ used here.

We utilize here again the bag model equation of state in the deconfined phase. The hadronic part is modelled as massless ideal gas with 3 or 6.68 [12] effective degrees of freedom. The increased number of degrees of freedom 6.68 is aimed at a check of the reduced latent heat (see ref. [12] for details), which is diminished by 50% in comparison with the standard bag model with 3 massless pions. Such a reduced latent heat is in line with recent lattice calculations near T_c [18].

In fig. 5 the invariant mass spectra are displayed for various diphoton sources. We

employ here the equation of state with reduced latent heat. As can be observed in fig. 5 the thermal spectrum at $M > 1$ GeV is dominated by the quark fusion process. Around $M = 1$ GeV the pion annihilation can contribute noticeably to the total yield. The relative contribution of the gluon fusion process to the overall diphoton yield depends on the chemical equilibration velocity; for the fast equilibration employed here we estimate at $M = 1$ - 3 (3 - 5) GeV roughly 10 (30)% from gluon fusion. Therefore, due to the assumed rapid chemical equilibration the gluon channel does not play an important rôle. (Only at very large values of $M > 10$ GeV the gluon contribution is as large as the quark annihilation process.) At $M = 1$ - 3 GeV the gluon channel could become significant if the chemical equilibration would proceed extremely slowly so that up to T_c the relation $\lambda_q = \frac{1}{5}\lambda_g$ would be valid. In our model, however, we assume fast equilibration and the difference between λ_q and λ_g is rapidly diminished. We mention that the down-extrapolated Drell - Yan like process dominates over the thermal yield at $M > 2.3$ GeV. If we use the standard bag model equation of state with a massless pion gas below T_c, the crossing of the Drell - Yan yield and the thermal yield does not change noticeably, however, the hadron contribution then becomes the main source at $M < 1.2$ GeV due to the longer stay of the thermal medium at T_c.

The dominance of the diphoton radiation off deconfined matter implies the $M_\perp$ scaling, i.e., the independence of $dN/dM_\perp\, dq_\perp^2\, dY$ on $q_\perp$ at fixed $M_\perp$ [12, 33]. Due to the logarithmic dependence of the scaled cross sections $\sigma^{(i)}(M^2)\, M^2$ in the high invariant mass region, there appears only a weak violation of the $M_\perp$ scaling of diphotons from deconfined matter. As shown in fig. 6a the $M_\perp$ scaling is nicely obtained in a wide region of $q_\perp$ at transverse mass $M_\perp = 2.6$ GeV because of a dominant contribution from deconfined matter. As demonstrated for dileptons [12] the standard bag model equation of state causes a sizeable transverse expansion of hadronic matter (due to the large latent heat which allows for a longer life time of the system). This might violate the $M_\perp$ scaling in the small M region, where the hadron source becomes dominating (see fig. 6b). The $M_\perp$ scaling might therefore serve as useful tool to check whether deconfined matter shines out. A strong violation in the region $q_\perp \to M$ can also be exploited as signal of collective transverse expansion.

5 Discussion and summary

In summary we present estimates of the diphoton spectra from thermalized matter which is expected to result in central collisions of lead nuclei at SPS and RHIC energies. At SPS energies we explore two different scenarios: with and without deconfinement transition. While for the first one we utilize the standard bag model equation of state, we model in the second one a hadron gas as mixture of ideal gases of the 100 lightest hadrons and resonances. For both scenarios we get rather similar slopes of the diphoton spectra, reflecting approximately the same initial temperature of the hot matter, and an increase of the yield due to deconfinement effects. These conclusions are in contrast to previous considerations in ref. [15], where extremely high temperatures of the hadron gas are obtained. Unfortunately, a chance to observe thermalized matter at SPS energies by using the diphoton invariant mass spectra alone turns out to be rather small. This is mostly due to the Drell - Yan like process which dominates the rate down to $M = 1.5$ GeV. In this region also soft processes and hadron decays might become significant which need separate consideration.

For RHIC energies our dynamical model includes the chemical equilibration process in the initially gluon-rich parton matter. We find that there seems to be a favorable window in the diphoton spectra below $M = 2.5$ GeV where deconfined matter can possibly be seen. This result can be confirmed by the $M_\perp$ scaling behavior which can serve as signal for a significant contribution from deconfined matter which does not undergo strong transverse expansion.

We do not include in our analysis pre-equilibrium contributions [34, 35]; due to strong correlations of phase space and space-time of initial partons it is expected to be less important [36].

The experimental analysis of diphoton spectra might serve as complementary to the dilepton and single-photon spectra to understand the dynamics of strongly interacting matter in the course of ultrarelativistic heavy-ion collisions. However, the discrimination of competing background from Drell - Yan like production and uncorrelated pairs is needed and represents a difficult task. We expect that the specific angular dependence [37] and relative momentum spectra can increase the abilities to select the wanted signal from thermalized matter. Despite the fact that diphotons at $M \gtrsim 1$ GeV are probably hard to measure, they represent an interesting tool to test thermalization and it is expected that the observation of $\gamma\gamma$ pairs can shed some light on chiral symmetry restoration and

deconfinement effects in heavy-ion collisions.

Acknowledgments

This work is supported by BMBF (grant 06DR666), DFG and GSI. Useful discussions with L. Razumov, M. Thoma, and G. Zinovjev are gratefully acknowledged. B.K. and K.R. thank J. Cleymans for the warm hospitality during their stay at the university of Cape Town, where this work has been started. O.P.P. thanks the nuclear theory group in the Research Center Rossendorf for the warm hospitality. K.R. acknowledges partial support from the committee of research development (KNB) under grand 001 and GSI for support and kind hospitality.

References

[1] I. Tserruya: *Nucl. Phys.* A 590 (1995) 127.

[2] G. Agakichiev et al. (CERES colloboration): *Phys. Rev. Lett.* 75 (1995) 1272.

[3] R. Albrecht et al. (WA80 collaboration): *Phys. Rev. Lett.* 76 (1996) 3506.

[4] D.K Srivasta, B. Sinha: *Phys. Rev. Lett.* 73 (1994) 2421,
D.K. Srivastava, B. Sinha, C.Gale: *Phys. Rev.* C 53 (1996) R567.

[5] W. Cassing, W. Ehehalt, C.M. Ko: *Phys. Lett.* B 363 (1995) 35.

[6] G.Q. Li, C.M. Ko, G.E. Brown: *Phys. Rev. Lett.* 75 (1995) 4007

[7] H.J. Schulz, D. Blaschke: preprint Univ. Rostock (1996) *Phys. Lett.* in print

[8] R. Baier, K. Redlich: Proc. "Hadrons in Dense Matter", GSI meeting, Darmstadt 1996, to be published,
R. Rapp, J. Wambach: ibid,
K. Haglin: ibid, *Phys. Rev.* C 53 (1996) R2606,
C. Song, V. Koch, S. Lee, C.M. Ko: *Phys. Lett.* B 366 (1995) 379.

[9] R. Yohida, T. Miyazaki, M. Kadoya: *Phys. Rev.* D 35 (1987) 388.

[10] K. Redlich: *Phys. Rev.* D 36 (1987) 3378.

[11] B. Kämpfer, O.P. Pavlenko: *Z. Phys.* C 42 (1994) 491.

[12] B. Kämpfer, O.P. Pavlenko, A. Peshier, G. Soff: *Phys. Rev.* C 52 (1995) 2704.

[13] J. Alam, D.K. Srivastava, B. Sinha, D.N. Basu: *Phys. Rev.* D 48 (1993) 1117.

[14] B. Datta, S. Raha, B. Sinha: *Nucl. Phys.* A 490 (1988) 733,
J. Letessier, A. Tounsi: *Phys. Rev.* D 40 (1988) 2914.

[15] D.K. Srivastava, B. Sinha, T.C. Awes: preprint (1996).

[16] E.V. Shuryak: *Phys. Rev. Lett.* 68 (1992) 3270,
P. Levai, B. Müller, X.N. Wang: *Phys. Rev.* C 51 (1995) 3326,
K. Geiger: *Phys. Rep.* 258 (1995) 237,
X.N. Wang: hep-ph/9605214, *Phys. Rep.* in print.

[17] T.S. Biro, E. van Doorn, B. Müller, M.H. Thoma, X.N. Wang: *Phys. Rev.* C 48 (1993) 1275.

[18] G. Boyd, J. Engels, F. Karsch, E. Laermann, M. Lütgemeier: PRL 75 (1995) 4169.

[19] J. Badier et al. (NA3): *Phys. Lett.* B 164 (1985) 184.

[20] L.V. Razumov, H. Feldmeier: preprint GSI-95-46, *Phys. Lett.* in print.

[21] R. Baier, H. Nakkagawa, A. Niégawa, K. Redlich: *Phys. Rev.* D 45 (1993) 4323.

[22] R. Baier, H. Nakkagawa, A. Niégawa, K. Redlich: *Z. Phys.* C 53 (1992) 433.

[23] J. Kapusta, P. Lichard, D. Seibert: *Phys. Rev.* D 44 (1992) 2774.

[24] Ch. Traxler, M. Thoma: *Phys. Rev.* C 53 (1996) 1348.

[25] A. Peshier, B. Kämpfer, O.P. Pavlenko, G. Soff: *Phys. Lett.* B 337 (1994) 235, A. Peshier, B. Kämpfer, O.P. Pavlenko, G. Soff: FZR-106 (1995), *Phys. Rev.* D (1996) in print.

[26] R.D. Field: Applications of perturbative QCD. Redwood City: Addison - Wesley Publishing Company 1989.

[27] R. Vogt, B.V. Jacak,P.L. McGaughey, P.V. Ruuskanen: *Phys. Rev.* D 49 (1994) 3345.

[28] S. Gavin, S. Gupta, R. Kauffman, P.V. Ruuskanen, D.K. Srivastava, R.L. Thews: *Int. J. Mod. Phys.* A 10 (1995) 2961.

[29] A. Dumitru, D.H. Rischke, Th. Schönfeld, L. Winckelmann, H. Stöcker, W. Greiner: *Phys. Rev. Lett.* 70 (1993) 2860.

[30] B. Kämpfer, O.P. Pavlenko, M.I. Gorenstein, A. Peshier, G. Soff: *Z. Phys.* A 353 (1995) 71.

[31] B. Kämpfer, O.P. Pavlenko: *Phys. Lett.* B 255 (1991) 503.

[32] B. Müller: invited talk at the workshop "The quark, the plasma, and beyond", Bielefeld, 1996.

[33] L. McLerran, T. Toimela: *Phys. Rev.* D 31 (1985) 545.

[34] B. Kämpfer, O.P. Pavlenko: *Phys. Lett.* B 62 (1992) 127.

[35] K. Geiger, J.I. Kapusta: *Phys. Rev. Lett.* 70 (1993) 1920,
K. Geiger: *Phys. Rev. Lett.* 71 (1993) 3075.

[36] Z. Lin, M. Gyulassy: *Phys. Rev.* C 51 (1995) 2177.

[37] S. Hirasawa, M. Kadoya, T. Miyazaki: *Phys. Lett.* B 218 (1989) 263.

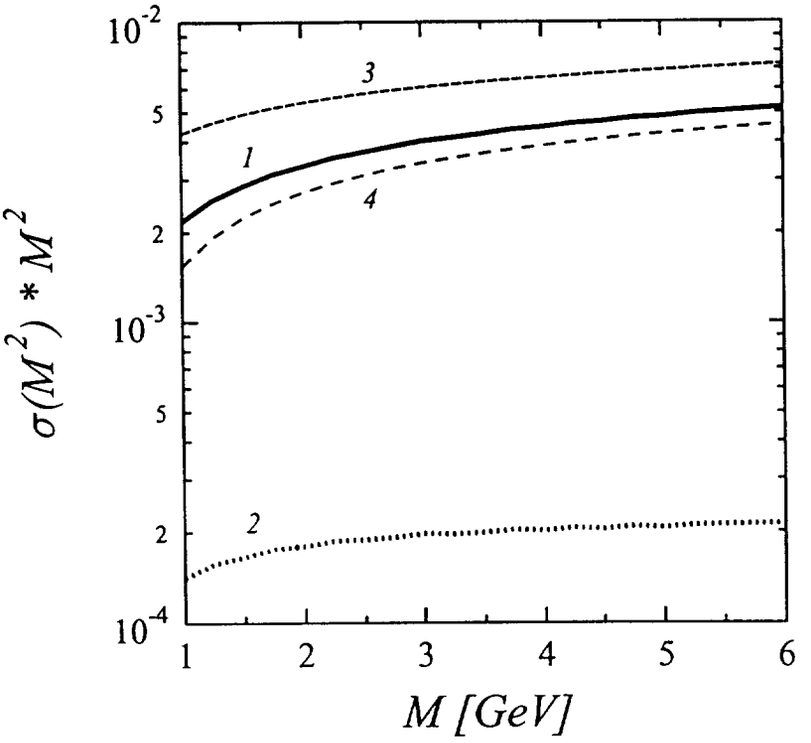
10^{-2}
5
2
10^{-3}
5
2
10^{-4}
1
2
3
4
5
6
3
1
4
2
$\sigma(M^2) * M^2$
M [GeV]

Fig. 1a

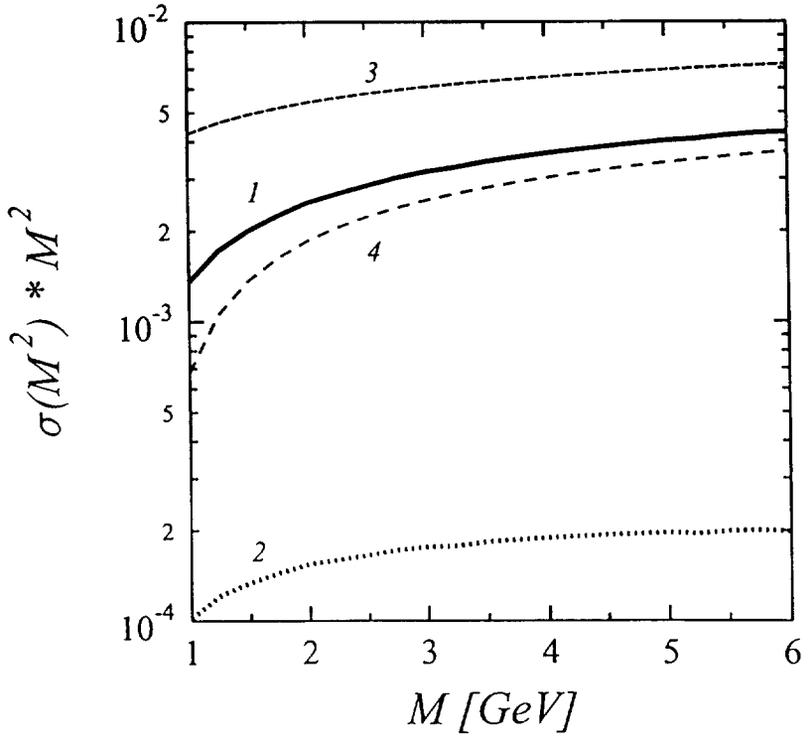
10^{-2}
5
2
10^{-3}
5
2
10^{-4}
1
2
3
4
5
6
3
1
4
2
$\sigma(M^2) * M^2$
M [GeV]

Fig. 1b

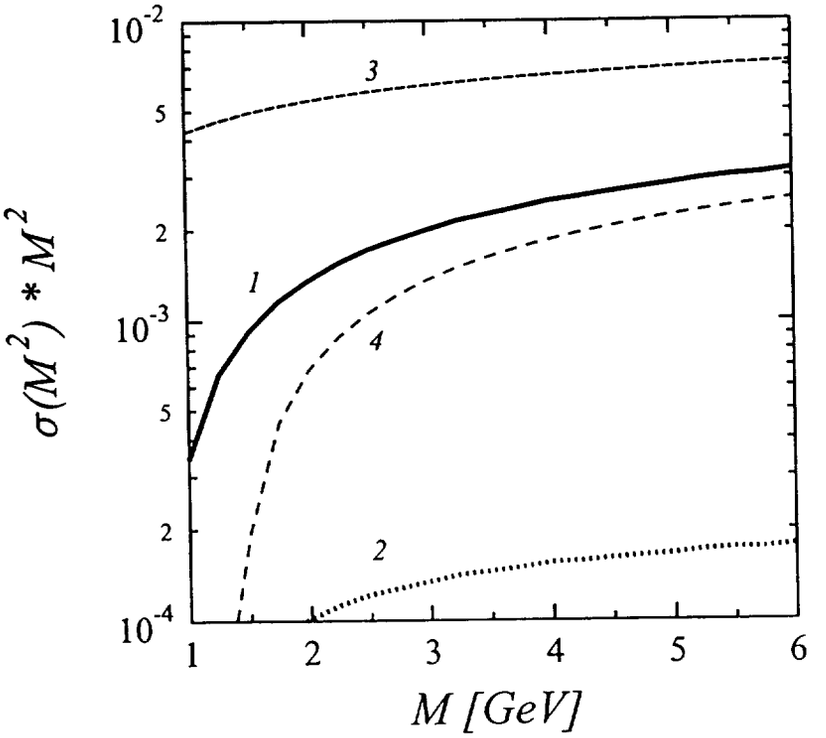

Fig. 1c

Fig. 1: Dimensionless scaled diphoton cross sections described in the text (1: $\sigma^{q\bar{q}\to\gamma\gamma}$, 2: $\sigma^{gg\to\gamma\gamma}$, 3: $\sigma^{q\bar{q}\to\gamma\gamma}_{m_q^0}$, 4: $\sigma^{q\bar{q}\to\gamma\gamma}_{T}$) as function of the invariant mass at various temperatures (a: $T = 150$ MeV, b: $T = 250$ MeV, c: $T = 500$ MeV). Curves 1 and 2 rely on full phase space saturation, i.e., $\lambda_{q,g} = 1$.

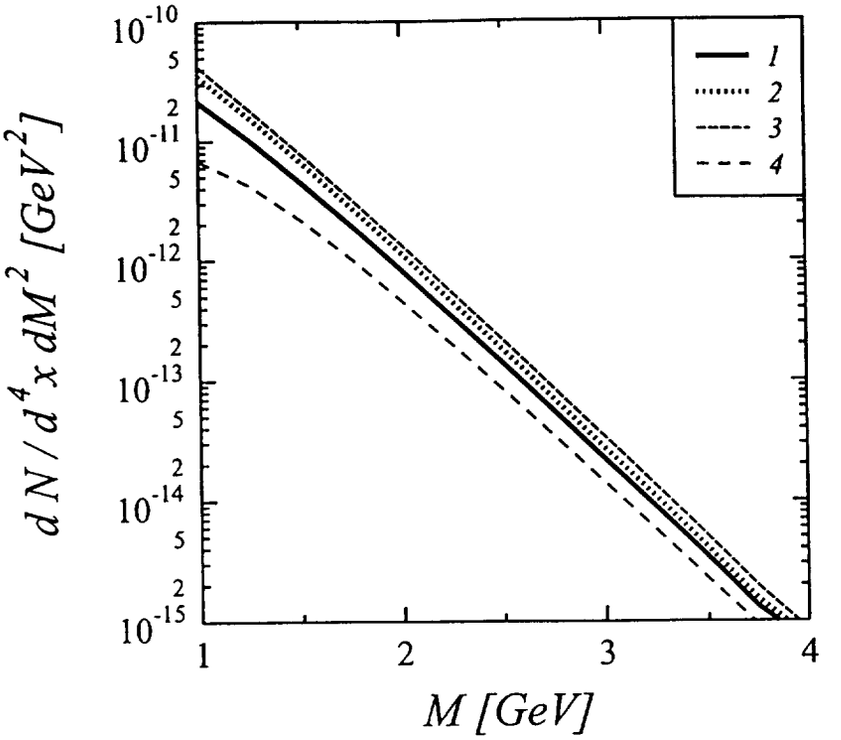

Fig. 2a

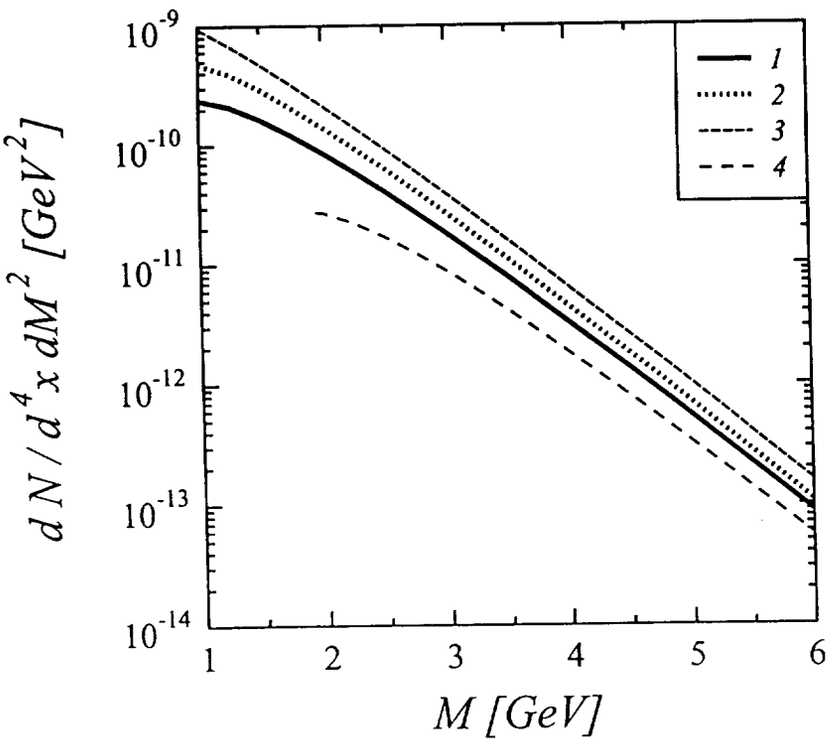

Fig. 2b

Fig. 2: The diphoton rates eq. (6) as function of the invariant mass for two temperatures (a: $T = 250$ MeV, b: $T = 500$ MeV) and $\lambda_g = 0.5$ and $\lambda_q = \frac{1}{5}\lambda_g$ (the meaning of the curves is as in fig. 1).

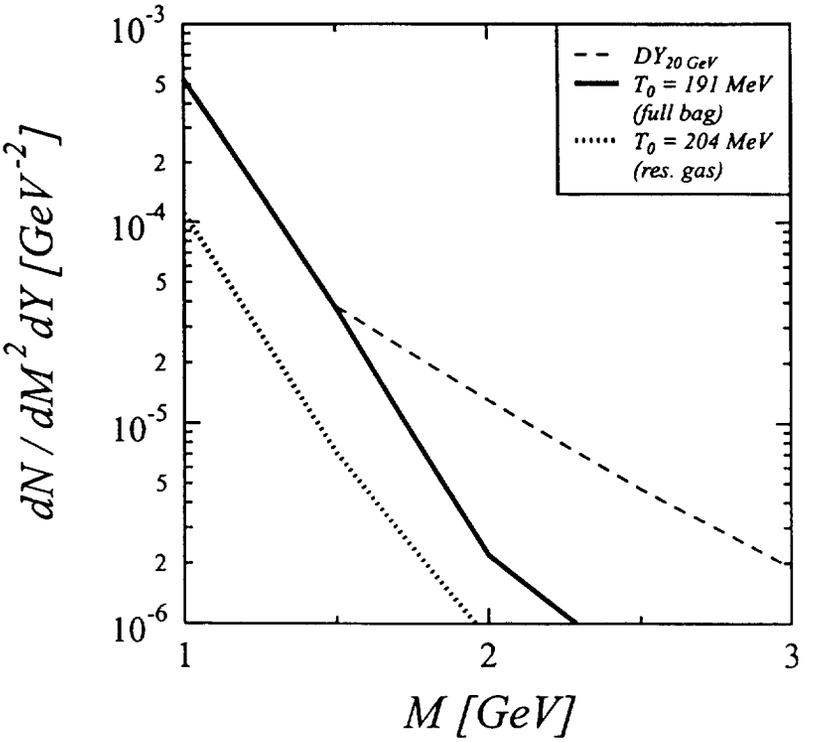

Fig. 3: Invariant mass spectra (total thermal yields) of diphotons for the scenarios I (standard bag model) and II (resonance gas). The initial temperatures correspond to the charged-particle rapidity density $dN_{ch}/dY = 410$ or initial entropy density $s_0 = 0.11$ GeV^3. The down-extrapolated Drell - Yan like yield for $\sqrt{s} = 20$ GeV is scaled by $200^{4/3}$.

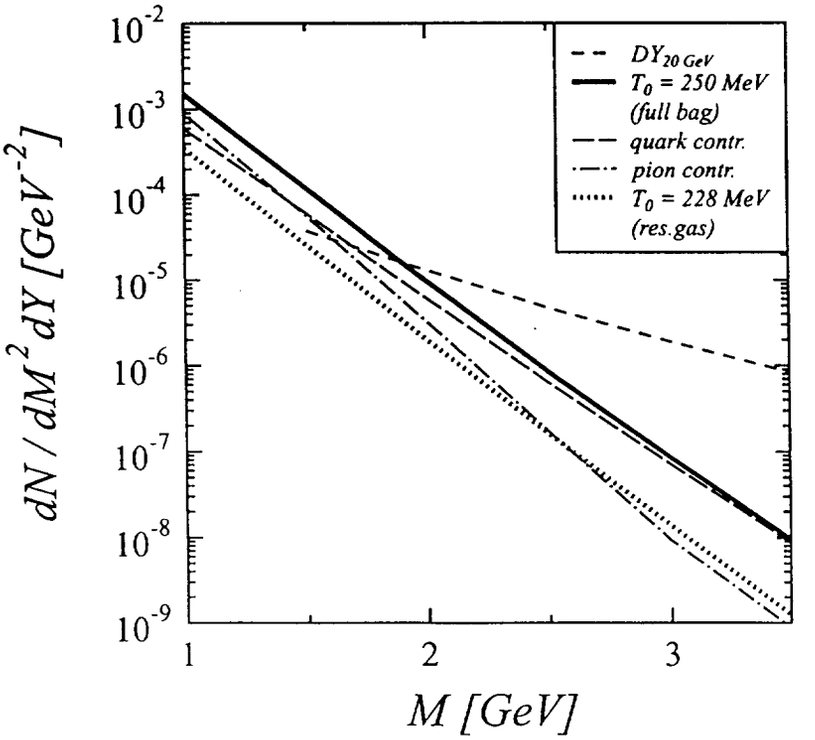

Fig. 4: The same as in fig. 3, but for higher initial temperatures which correspond to $s(T_0) = 0.25$ GeV^3. The individual contributions (including pure and mixed phases) for scenario I are displayed separately. The Drell - Yan like yield is as in fig. 3.

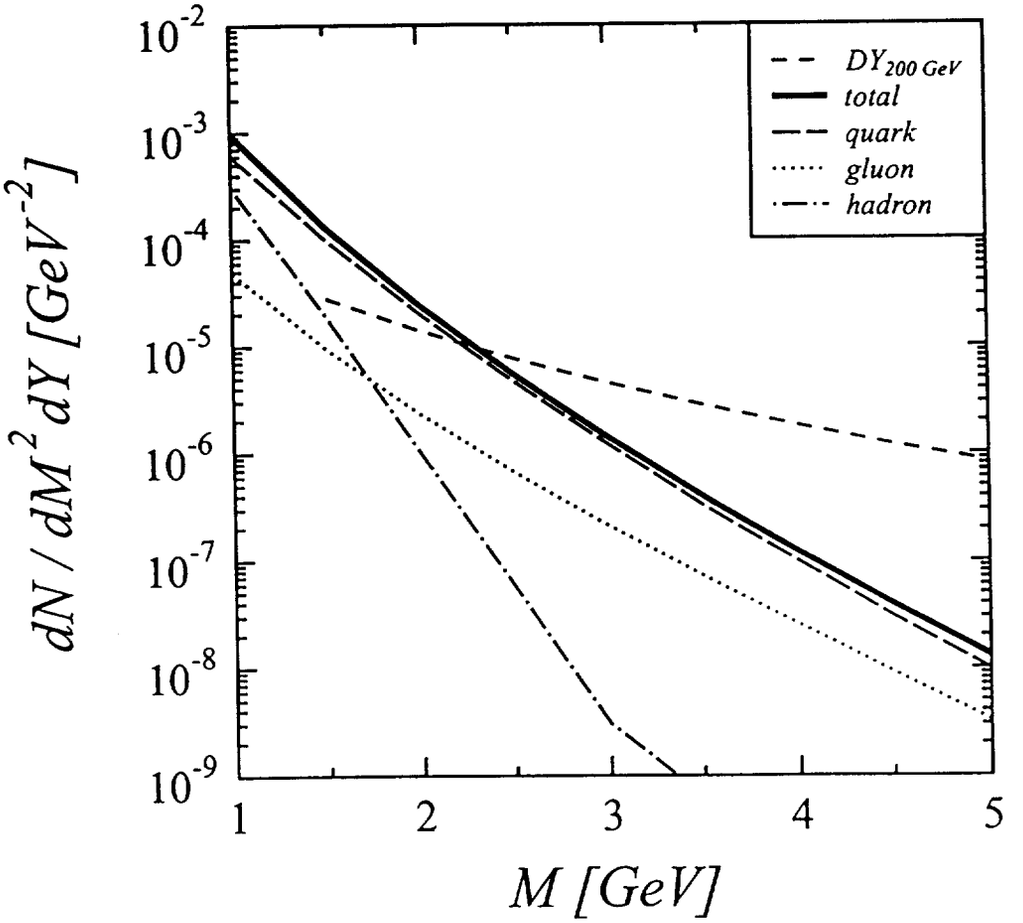

Fig. 5: Invariant mass spectrum of diphotons for $T_0 = 550$ MeV and $\lambda_g^0 = 0.5$. The down-extrapolated Drell - Yan like yield for $\sqrt{s} = 200$ GeV is scaled by $200^{4/3}$.

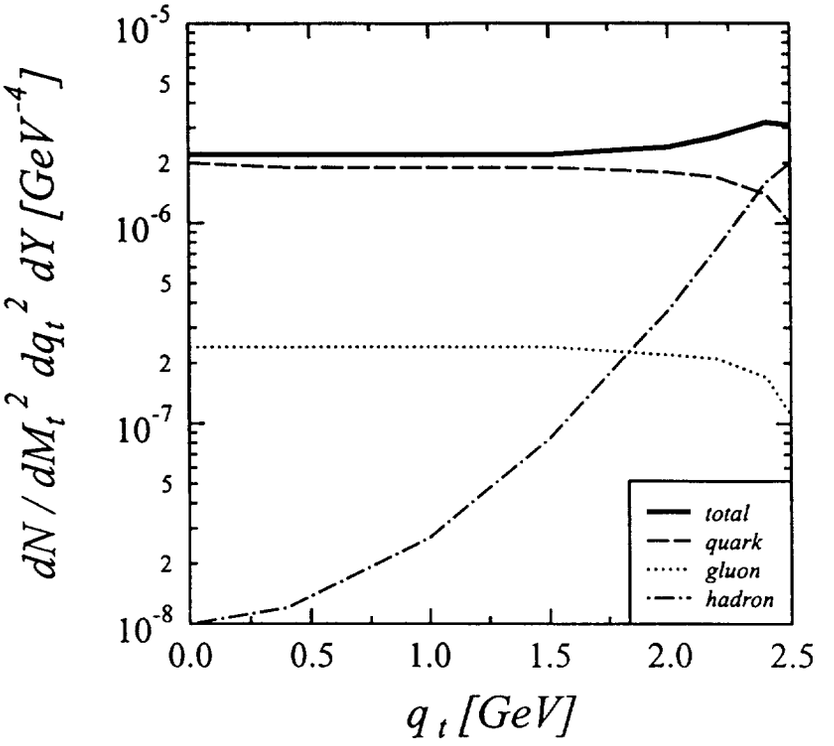

Fig. 6a

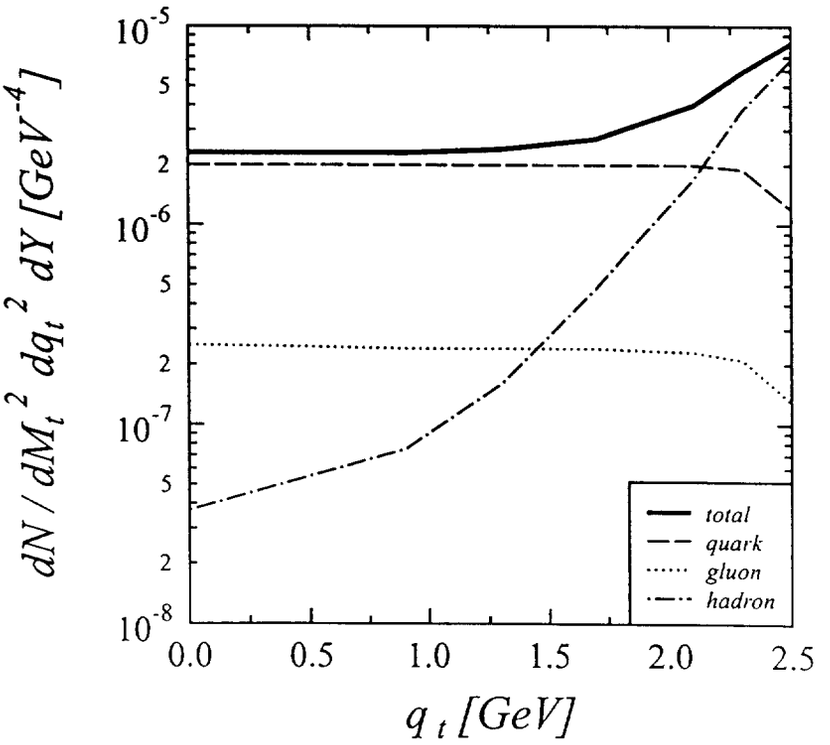

Fig. 6b

Fig. 6: Transverse momentum spectrum of diphotons for RHIC conditions for transverse pair mass $M_\perp = 2.6$ GeV (a: equation of state with reduced latent heat, b: standard bag model equation of state). Notation and initial conditions as for fig. 5.